Creep Behaviour of Steel Bonded Joints under Hygrothermal Conditions

Chantal de Zeeuw[1], Sofia Teixeira de Freitas[1], Dimitrios Zarouchas[1], Markus Schilling[2], Romina Lopes Fernandes[1], Pedro Dolabella Portella[2], and Ute Niebergall[2]

[1]Structural Integrity & Composites Group, Faculty of Aerospace Engineering, Delft University of Technology, Netherlands

[2]Mechanics of Polymers Division, Materials Engineering Department, Bundesanstalt für Materialforschung und -prüfung, Berlin, Germany

Abstract

The aim of this research is to study the influence of moisture absorption at low moisture contents on the creep behaviour of an epoxy adhesive in steel bonded joints. Single lap joints were manufactured using high strength steel adherends and a two-component epoxy adhesive. The single lap joints were tested at load levels corresponding to average lap shear stresses of ± 5%, 15%, 30% and 45% of the dry lap shear strength in both 40°C air and 40°C distilled water. Specimens were not pre-aged to be able to analyse the coupled effect of moisture and loading. The test results show that an increase in the load level resulted in an increase in the instantaneous strain and in the creep strain rate. The creep strain of single lap joints loaded in water was generally larger than for the ones loaded in air. For joints loaded in water the creep behaviour was found to be dependent on the moisture concentration in the adhesive. At low moisture percentages creep was suppressed, resulting in a lower instantaneous strain. At higher moisture percentages creep was promoted, resulting in a larger strain rate. The suppression of creep at low moisture percentages is attributed to water molecules bonding to the epoxy macromolecules, resulting in a reduction in molecular mobility and a smaller creep strain. At higher moisture percentages the plasticizing effect of the water dominates, resulting in a larger creep strain. The Maxwell three-element solid model and Kelvin-Voigt three-element solid model were used to simulate the creep behaviour of the single lap joints loaded in air and water. The models gave good representations of the creep response across the different load levels in both water and air, they were however unable to give a correct representation of the instantaneous strain of the single lap joints loaded in water. This is attributed to the models being unable to account for the present short-term relaxation process that is dependent on the moisture concentration.

Keywords C. lap-shear, D. aging, D. creep D. viscoelasticity, hygrothermal, viscoelastic model

1 Introduction

Structural adhesives are increasingly being used in aerospace, maritime and automotive applications for their specific benefits when compared to more traditional mechanical fastener methods such as bolts or rivets. Papanicolaou et al. [1] mentioned that these benefits include the minimization of stress concentrations, the distribution of stresses over a larger area and a reduction of the overall weight. Adhesives do however exhibit viscoelastic behaviour and will experience creep deformation when subjected to a constant load. Papanicolaou et al. [2] noted that creep is among the main causes for damage development in polymers. The relevance of studying creep is further emphasized by the remark of Ashcroft & Briskham [3] that for most structures creep loading will be present in its load spectra. Another important factor in damage development in polymers mentioned by Papanicolaou et al. [2] is water absorption or moisture. The absorbance of water will result in a stiffness and strength decrease and will also cause an increase in the creep strain. This results in a combined creep and moisture effect damaging the polymer material when used in maritime and offshore applications. It is therefore important to get a good understanding of the influence of moisture on the creep behaviour of adhesively bonded joints subjected to combined moisture and loading conditions.

Springer & Wang [4] creep tested adhesively bonded single lap joints immersed in water. Before testing, the specimens were pre-conditioned in humid air (50% relative humidity), distilled water or a 5% NaCl-distilled water solution for two months. During these two months, the temperature was kept constant at either 23°C or 93°C . The specimens were dried before being creep tested at 10%, 20% or 30% of the lap shear strength. During creep tests the specimens were exposed to the same environment as during preconditioning. The creep behaviour was found to depend on the applied load, the environment and the temperature. An increase in the load or temperature resulted in an increase in the creep. Specimens exposed to water experienced more creep than specimens exposed to 50% humidity, while the creep for specimens immersed in the 5% NaCl-distilled water solution was similar to the creep of specimens immersed in distilled water. Gellert & Turley [5] studied combined moisture and loading by immersing 7 mm thick glass fibre reinforced laminates with different resins (vinylester, polyester and phenolic) in 30^{o}C seawater while loading them at 20% of the maximum strain at flexural failure under four-point loading. The specimens were periodically withdrawn to determine the creep strain. The results from these tests were compared to specimens loaded under atmospheric conditions. The immersed specimens experienced up to double the creep strain of their atmospherically aged counterparts. Guedes et al. [6] and Farshad & Necola [7] looked at the effect of moisture on the creep behaviour of glass fibre-reinforced polyester pipes. They creep tested composite pipe specimens by applying a constant dead weight. During testing the specimens were submerged in water at room temperature. This loading configuration simulates the external loads induced in sub-soil installation [6]. Farshad & Necola [7] preconditioned some of their ring samples in 20°C water for at least 1000 hours before testing and found that exposure to water mainly affected the strength of composite ring specimens, the maximum creep strain did not vary much. Guedes et al. [6] preconditioned some of their specimens in 50°C water and found that preconditioning had a small influence on the initial stiffness. The creep behaviour of the preconditioned specimens was similar to that of the unconditioned specimens. Feng et al. [8] creep tested two epoxy adhesive systems at different temperatures under dry condition and at 95% relative humidity (wet condition). The samples tested in the wet condition were preconditioned until they reached the saturation level. They found that the creep compliance reached its limit, the equilibrium compliance, up to 1000 times faster in wet conditions than in dry conditions. This accelerates the creep behaviour with the presence of water. Subjecting the specimens to a higher temperature or to moisture both led to more pronounced creep behaviour. Feng et al. [8] therefore suggest that the presence of absorbed moisture can result in the same creep response as a higher temperature in the dry condition. The main finding of previous studies can be summarized as follows: the creep strain of specimens subjected to moisture is larger than that of unconditioned (dry) specimens.

Most of the previous studies preconditioned their specimens for a set time or until saturation before testing. Dean [9] compared the creep behaviour of epoxy adhesive specimens stored in a desiccator for three months to specimens stored in a laboratory under ambient conditions for eight weeks. By doing this, they showed that even a small amount of absorbed water can influence the creep deformation of epoxy adhesives. By starting with a specimen that has already been preconditioned it is not possible to study the interaction between the moisture absorption and creep. The work by Gellert & Turley [5] compared the creep strain of beams loaded under combined moisture and loading with the creep strain of beams loaded under atmospheric conditions. Their first datapoint for the creep strain is however after 7 days of combined moisture and loading and therefore again does not give an idea of the interaction between the moisture absorption and creep in the early stages of water uptake.

In this study the focus is on the combined effect of moisture and loading on the creep behaviour of an epoxy adhesive in steel bonded single lap joints at low moisture concentrations (early stages of water uptake). By combining the moisture and loading it is possible to study the interaction between moisture absorption and creep. Single lap joints have been subjected to combined moisture and loading at different load levels. Various viscoelastic models are compared on their ability to simulate the creep response of the single lap joints in water and air at different load levels.

2 Materials and specimens

Single lap joints were manufactured by bonding two steel adherends using an epoxy adhesive. The substrate material used was S700MC steel. The adhesive was Araldite 2015 (Huntsman, United States [10]), a two-component epoxy paste adhesive. The dimensions of the final joint are shown in **Figure 1**. The dimensions of the joint were based on the available grips and environmental chambers that were used during testing.

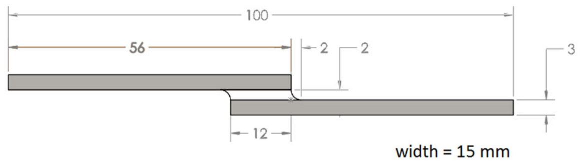

Figure 1: Configuration of steel-to-steel single lap joints (dimensions in mm).

The bonded areas were pre-treated mechanically and chemically before bonding. First, surfaces were sand blasted and cleaned using a clean cloth with acetone. Afterwards, a silane treatment was applied as an adhesion promoter. The silane coupling agent that was used is Silquest A-187 epoxy silane (γ- glycidoxypropyltrimethoxysilane [γ-GPS],Momentive, United States [11]). The silane pretreatment used is based on the work by Abel et al. [12] and is a 1% solution of silane with distilled water. The silane solution was hydrolyzed for one hour under continuous stirring in distilled water with a natural pH of 5-6 and was then applied within 15 minutes to the bond area using a clean brush. The surface was kept wet for ten minutes before substrates were placed vertically on a paper towel to allow the absorption of excess silane solution by the paper. Substrates were then left to dry at room temperature for one hour.

The bonding process was performed with the help of an alignment mould – see **Figure 2** The use of the mould ensures that specimens are always properly aligned and helps to achieve a consistent bond line thickness. The way the mould was designed also results in consistent 2 by 2 mm 45° fillets on the lap joints - see **Figure 3**. The mould with the bonded substrates was placed inside an 80°C oven for 2 hours. A thermocouple was placed in the adhesive to monitor the temperature of the adhesive during curing. However, the intended curing period and temperature of the adhesive of 1 hour at 80°C was not reached in the first curing cycle. Therefore, specimens were later post-cured in a 90°C oven for three hours. This was done to ensure the specimens were fully cured and there would not be a reactivation of curing caused by the ingress of water as has for example been observed by Papanicolaou et al. [2].

The used cure cycle of 1 hour at 80°C is based on DSC experiments performed on the adhesive. **Figure 4** shows the program temperature cycle. Samples of the adhesive were heated from 20°C to 80°C at a rate of 10°C/min. The temperature was held at 80°C for 60 minutes before being cooled to 20°C again at 2°C/min. The program was run twice with the same specimen. **Figure 5** presents the heat flow vs time for both the first and the second test. The start

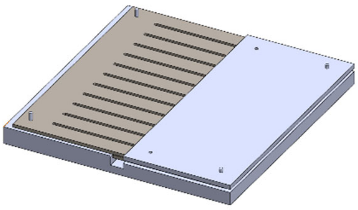

Figure 2: Alignment mould

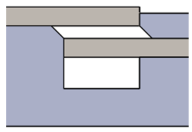

Figure 3: Detail of alignment mould

of the graphs corresponds with the heat-up of the sample. The heat flow for the first test becomes positive once the curing process starts to release heat. It becomes negative again once the energy required to keep the sample at 80°C is higher than the amount of energy released by the curing process. Finally, the heat flow levels out at a constant negative value. This is the amount of energy necessary to keep the sample at 80°C. At this point the adhesive can be considered fully cured. For the second test there is a straight line after the heat-up stage. This shows that the sample was already fully cured during the initial cycle of the experiment.

After curing, sandpaper was used to shape the 2 by 2 mm 45° fillets to fillets with a radius of 2 mm, as shown in **Figure 1**. The steel adherends were cleaned and coated using two layers of "Hammerite No.1 Rust Beater" and four layers of "Hammerite Direct to Rust Metal Paint" to protect them against rust while immersed in the water.

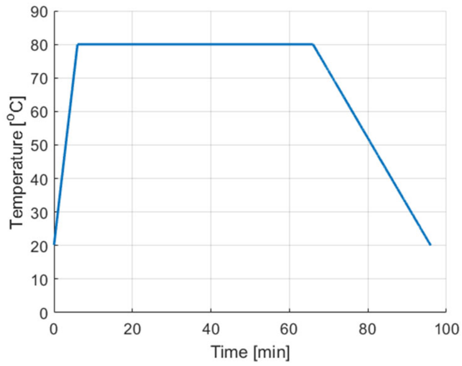

Figure 4: Program temperature vs time for DSC tests

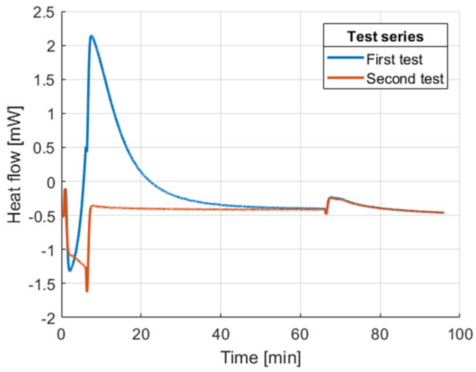

Figure 5: Heat flow vs time for DSC tests

3 Experimental Procedure

During the experiments, single lap joint specimens were subjected to a constant tensile load for up to 14 days (creep load). Experiments were carried out both in air and in distilled water at 40°C. The experiments in air were used as a reference for the experiments in distilled water. Distilled water was chosen because literature shows that distilled water results in worse ageing conditions in terms of water uptake than salt water, as can for example be seen in Zafar et al. [13]. The specimens were tested at four average lap shear stress levels: 1 MPa, 3 MPa, 6 MPa and 9 MPa. These average lap shear stress levels correspond to respectively 5%, 15%, 30% and 45% of the unaged lap shear strength, which was determined to be 20 MPa by de Zeeuw [14]. **Table 1** summarizes the experiments that have been conducted. Test series are labelled using a key that indicates the type of specimen (SLJ, single lap joint specimen), the test environment (A, air or W, water) and the load level (1 MPa, 3 MPa, 6 MPa or 9 MPa).

Table 1: Test matrix for creep experiments in air and water at elevated temperatures

Test series	Duration	Environment	Load	Sample size
SLJ_A_1MPa – Exp	14 days	40°C air	1 MPa	2
SLJ_A_3MPa – Exp	14 days	40°C air	3 MPa	2
SLJ_A_6MPa – Exp	4 days	40°C air	6 MPa	1
SLJ_A_9MPa – Exp	Until failure	40°C air	9 MPa	2
SLJ_W_1MPa – Exp	14 days	40°C distilled water	1 MPa	2
SLJ_W_3MPa – Exp	14 days	40°C distilled water	3 MPa	2
SLJ_W_6MPa – Exp	Until failure	40°C distilled water	6 MPa	1
SLJ_W_9MPa – Exp	Until failure	40°C distilled water	9 MPa	2

Experiments were carried out using Full Notch Creep Test [FNCT] equipment (Institut für Prüftechnik [IPT], Todtenweis, Germany) and the corresponding environmental chambers - see respectively **Figure 6a** and **Figure 6b**. The chambers were placed on a heating element and the temperature is controlled using a sensor in the chamber. The FNCT machine can control the applied load and temperature during testing and automatically records the creep deformation. During the experiments, the load was applied with an accuracy of ± 1 N and the temperature was controlled with an accuracy of ± 0.5°C. A pre-load of 20% was applied for 30 seconds, before the 100% set load value was applied to the specimens.

a) FNCT machine at the BAM

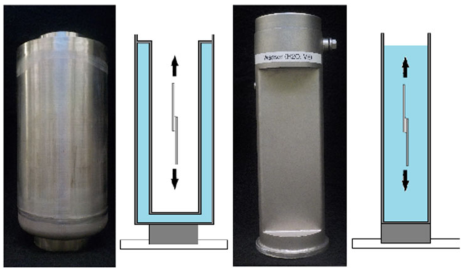

b) Environmental chambers

Figure 6: FNCT machine and environmental chambers (air (left) and fluids (right)) at the Bundesanstalt für Materialforschung und -prüfung [BAM].

4 Results

4.1 Experimental Results

For clarification when discussing the results, **Figure 7** shows a schematic of the different creep stages a viscoelastic material will go through when subjected to a constant and uniform load. The figure also indicates the instantaneous strain, ε_0, and strain rate, $\dot{\varepsilon}$. Depending on the magnitude of the load the instantaneous strain will either be fully elastic or elastic-plastic. The dashed line is the recovery curve, which shows the time-dependent decrease in strain upon removal of the load. The instantaneous decrease is equal to the elastic portion of the instantaneous strain. Creep strains will often not be fully recovered upon unloading, resulting in permanent strain. The total creep strain is therefore composed of a viscoelastic, recoverable, part and a viscoplastic, permanent, part [1, 3].

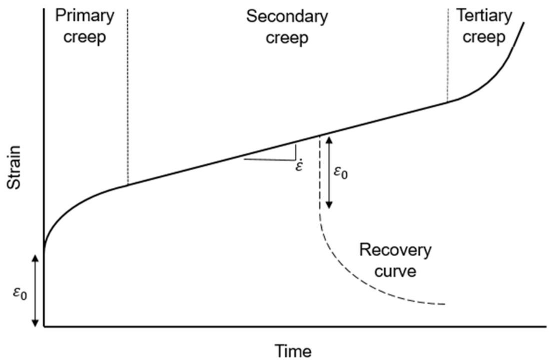

Figure 7: Creep curve for a viscoelastic polymer under constant stress and temperature. With instantaneous strain, ε_0, and strain rate, $\dot{\varepsilon}$.

Figure 8 and **Figure 9** present the creep results for the single lap joints loaded at 1 MPa, 3 MPa, 6 MPa and 9 MPa in air and water, respectively. All actual values are available publicly in the work by de Zeeuw [14]. The figures show that an increase in the load level results in a larger instantaneous strain, ε_0, and a larger strain rate, $\dot{\varepsilon}$.

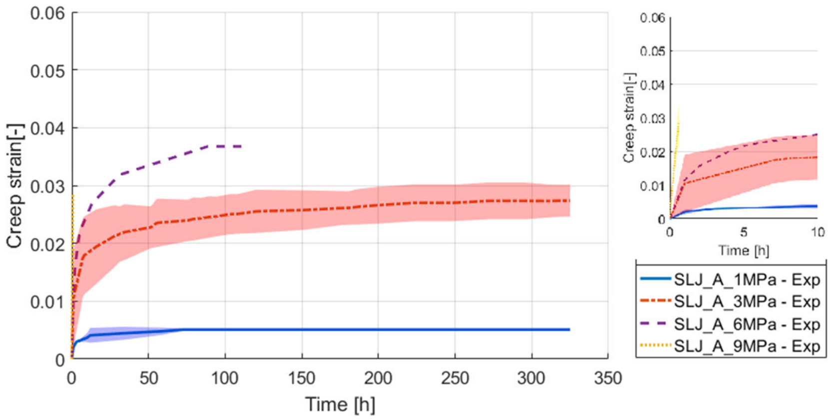

Figure 8: Creep strain of specimens loaded in 40°C air subjected to loads of 1 MPa, 3 MPa, 6 MPa and 9 MPa, Presented as the mean ± the standard deviation. For a colour version of this figure, the reader is referred to the online version of this journal.

Figure 10 presents the mean instantaneous strains and strain rates of **Figure 8** and **Figure 9**. The actual values for the graphs in **Figure 10** can be found in **Table 4** in Appendix 0. For 9 MPa no instantaneous strain is recorded because no obvious instantaneous strain was observed, no strain rate is recorded for 9 MPa in air because no obvious secondary creep stage was observed. **Figure 10a** shows that the instantaneous strain is not directly proportional to the load level. The instantaneous strain does however increase with an increase in the load level. For single lap joints loaded in water, the instantaneous strain is generally lower than the one for the same load level in air. For 6 MPa, the instantaneous strains observed in water and air are comparable. **Figure 10b** shows that the water has a significant effect on the strain rate and therefore on the viscoelastic response of the bonded joint. Single lap joints loaded in water experience a much larger strain rate than the ones loaded in air at the same load level. For specimens loaded at 1 MPa in air, the strain rate is very low: no significant amount of secondary creep is observed.

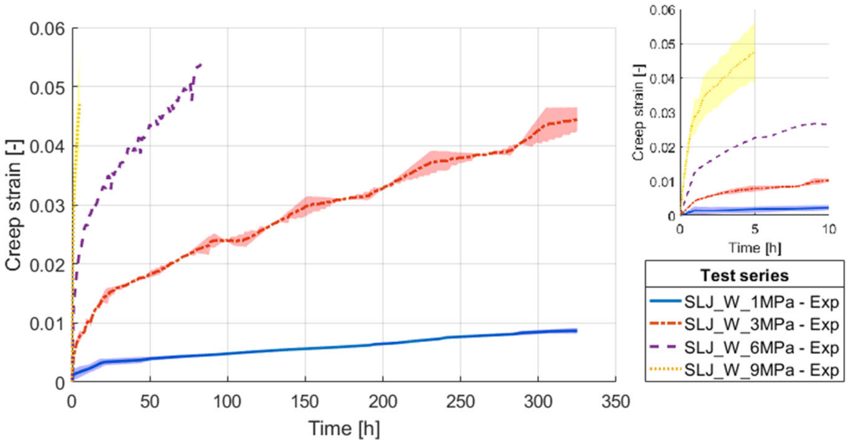

Figure 9: Creep strain for specimens loaded in 40°C distilled water subjected to loads of 1 MPa, 3 MPa, 6 MPa and 9 MPa, Presented as the mean ± the standard deviation. For a colour version of this figure, the reader is referred to the online version of this journal

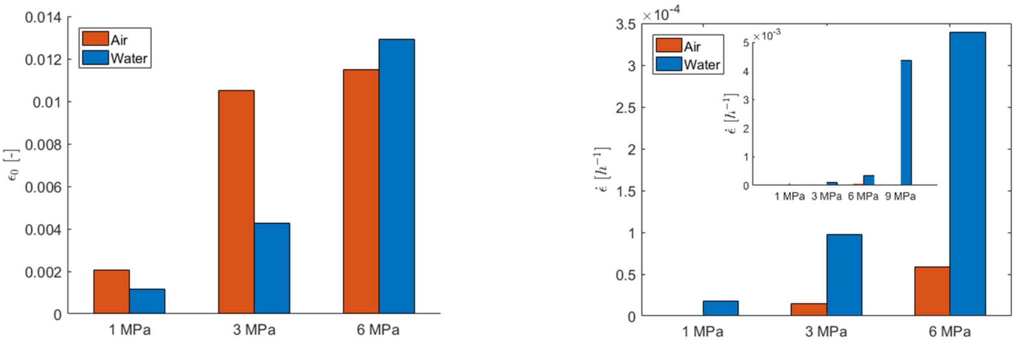

a) Mean instantaneous strain (ε_0)

b) Strain rate ($\dot{\varepsilon}$)

Figure 10: Variation in mean instantaneous strain and strain rate with load (1 MPa / 3 MPa / 6 MPa / 9 MPa) and loading condition (Air / Water). For a colour version of this figure, the reader is referred to the online version of this journal.

Figure 11a-Figure 11d compare the creep strains of specimens loaded in air and in water at the same load level. The individual creep curves can be found in **Figure 18** in Appendix B. As shown in **Figure 11a** and **Figure 11b**, during the initial hours of the experiments, the single lap joints loaded at 1 MPa and 3 MPa in water experienced a lower creep strain than specimens loaded at the same load level in air. Once the creep reaches the secondary creep stage, the creep of the specimens tested in water starts to become larger than the creep of the specimens tested in air. This is due to a higher strain rate $\dot{\varepsilon}$ - see **Table 4**. As shown in **Figure 11c,** the specimens loaded at 6 MPa experience a similar instantaneous strain in air and in water. The instantaneous strain is followed by a larger strain rate for the specimen loaded in water than for the specimen loaded in air. For 9 MPa (**Figure 11d**) the specimens loaded in water experienced a larger final creep strain and a longer time until failure than their air loaded counterparts.

These observations can be summarized as follows: for short time durations specimens loaded in water at 1 MPa, 3 MPa and 9 MPa were less prone to creep than specimens loaded in air. Later on in the experiment, the specimens loaded in water started to experience higher strain rates, resulting in a larger creep strain at the end of the experiment. This suggests that the influence of moisture on the creep response is dependent on the percentage of moisture in the adhesive. At the initial stages of water absorption (low moisture percentage) creep is suppressed while at later stages (higher moisture percentage) creep is promoted. No mention of this phenomenon has been found in literature.

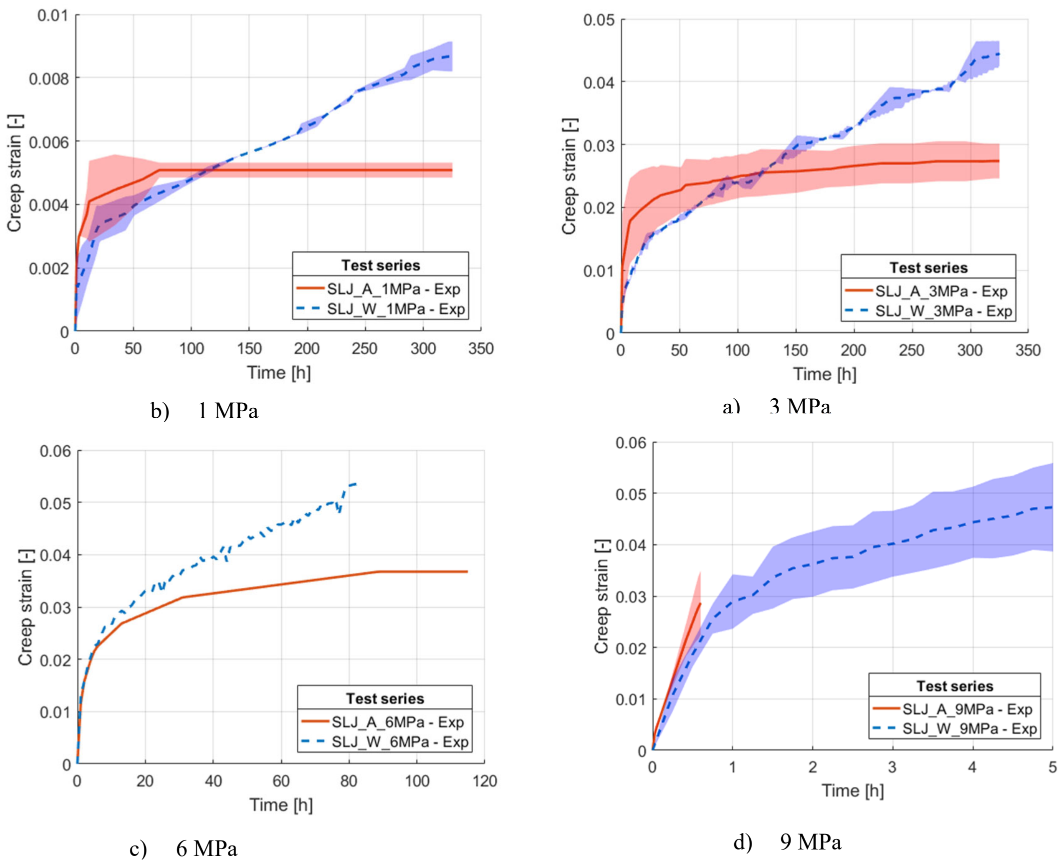

Figure 11: Creep strain for specimens loaded at 1 MPa, 3 MPa, 6 MPa and 9 MPa, Presented as the mean ± the standard deviation. For a colour version of this figure, the reader is referred to the online version of this journal.

4.2 Analytical Model

For this study, linear viscoelastic models that are made up of linear/Hookean springs and linear/Newtonian viscous dashpots in series and/or parallel have been used. The stress-strain relationships of spring and dashpot are respectively $\sigma = E \cdot \varepsilon_1$ and $\sigma = \eta \cdot \dot{\varepsilon_2}$, where E can be interpreted as the spring constant or a Young's modulus and η is the coefficient of viscosity [1, 3].

Feng et al. [8] noted that the parallel and series combinations of these two basic elements adequately fit experimental creep data, even for complicated composite materials. In general, adding more elements to the viscoelastic model will improve its accuracy in describing viscoelastic behaviour. The mechanical models are however all empirical models. The values of the elastic modulus and coefficient of viscosity are determined by varying them until the analytical curve closely matches the experimental curve. Since the deformation processes in viscoelastic materials are quite complex, it might be necessary to use different models for different loading conditions, as mentioned by Özkaya et al. [15].

In this study, the abilities of the Maxwell three-element solid model and the Kelvin-Voigt three element solid model to simulate the creep response of the single lap joint specimens in air and water are evaluated. These models give a simplified representation of the viscoelastic creep response to a load. They do not take plastic deformation into account and on the long-term scale the models will by definition lead to a zero strain rate. For the current work they were however found to give a good representation of the creep behaviour. In a previous study Ferrier et al. [16] used two Maxwell three-element models to model adhesive joints. Zehsaz et al. [17] used two Maxwell models and a spring in series with nonlinear functions of temperature and stress for the parameters to model the viscoelastic behaviour of a structural epoxy adhesive. The Kelvin- Voigt three-element model has been successfully used for the modeling of single lap joints by Groth [18] and Shishesaz & Reza [19] and for the modeling of adhesives in both the dry condition and after they had absorbed moisture by Dean [9]. The two-element Maxwell and Kelvin-Voigt model were also evaluated but were unsuccessful at accurately modeling the creep behaviour. They are therefore not included in this paper.

4.2.1 Maxwell three-element solid model

The first three-element solid model that will be discussed is the Maxwell three-element solid model. This model consists of a spring in series with a Maxwell model, as shown in **Figure 12**. This model gives bounded creep. The constitutive equation of the second three-element solid model can be found by using the constitutive equations of the spring and the Maxwell model ($\dot{\varepsilon} = \dot{\sigma}/E + \sigma/\eta$ [1]) and is as follows [20]:

$$\sigma + \frac{\eta_2}{E_2}\dot{\sigma} = E_1\varepsilon + \frac{\eta_2(E_1 + E_2)}{E_2}\dot{\varepsilon} \tag{1}$$

This constitutive equation can be rewritten to get the response of the model to a constant stress $\sigma = \sigma_0$, applied at t = 0:

$$\varepsilon = \frac{\sigma(E_2 t + \eta_2)}{E_1 E_2 t + \eta_2(E_1 + E_2)} \tag{2}$$

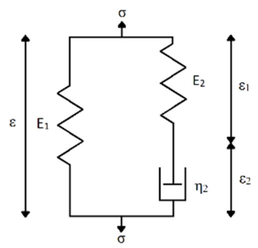

Figure 12: Maxwell three-element solid model.

This study used the Maxwell three-element solid model (**Figure 12**) to simulate the creep behaviour of the single lap joints. Non-linear regression was used to estimate the parameters E_1, E_2 and η_2 of the Maxwell three-element solid model based on the experimental data. Time was assumed as an independent variable and the creep strain ε_c was assumed as a dependent variable. **Table 2** presents the results for the different load levels and environment. **Figure 13** and **Figure 14** compare the experimental results with the results obtained using the three-element-solid model with the estimated parameters from **Table 2**.

Table 2: Parameters of the Maxwell three-element solid model

		η_2 [Pa · s]		E_1 [MPa]		E_2 [MPa]		R^2
		Estimate	Standard Error	Estimate	Standard Error	Estimate	Standard Error	
Air	1 MPa	948.09	24.00	191.60	0.25	367.11	21.44	0.9771
	3 MPa	1.49×10^3	34.22	105.88	0.21	131.39	3.43	0.9845
	6 MPa	1.29×10^3	38.98	152.46	0.59	333.25	15.63	0.9919
	9 MPa	176.42	2.83	33.08	4.04	4.97×10^3	262.09	0.9998
Water	1 MPa	3.68×10^4	1.60×10^3	27.67	3.10	366.00	4.60	0.9847
	3 MPa	1.52×10^4	446.42	29.45	1.09	268.49	5.20	0.9889
	6 MPa	3.80×10^3	297.86	78.36	3.08	267.37	11.07	0.9819
	9 MPa	168.15	12.93	162.21	3.70	6.36×10^3	9.45×10^3	0.9942

2

Table 2 shows that, for the single lap joints loaded in water, an increase in load results in a decrease in η_2. This is in line with what would be expected when looking at the response of the viscous dashpot to a load σ: $\varepsilon(t) = \sigma t/\eta$. A smaller value of η_2 will result in the same value of ε being reached in a shorter amount of time. For the specimens loaded in air there is this same pattern for load levels of 3 MPa, 6 MPa and 9 MPa. The η_2 value for 1 MPa is however lower than the values for 3 MPa and 6 MPa. This lower value is attributed to the load level being so low that there was no secondary creep. For E_1 there are clear differences between the single lap joints loaded in water and the ones loaded in air. For the air loaded specimens there is a general decrease in E_1 with an increase in σ. For the ones loaded in water an increase in the load level results in an increase in E_1. This suggests that the water causes a fundamental change in the behaviour of the spring corresponding to E_1 in the three-element solid model. The E_2 estimates show values of the same order of magnitude for 1 MPa - 6 MPa and much larger values for 9 MPa. This is attributed to the instantaneous strain of the specimens loaded at 9 MPa being significantly larger than at the lower load levels. **Table 2**, **Figure 13** and **Figure 14** show that the Kelvin-Voigt three-element solid model was able to give an accurate representation of the creep strain of the single lap joint specimens.

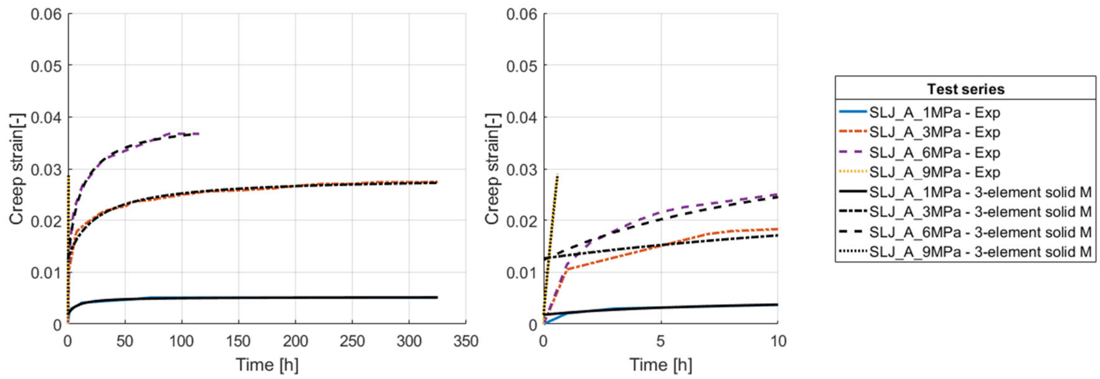

Figure 13: Experimental creep strain and creep strain simulated using Maxwell three element solid models for specimens subjected to loads of 1 MPa, 3 MPa, 6 MPa and 9 MPa in 40°C air. For a colour version of this figure, the reader is referred to the online version

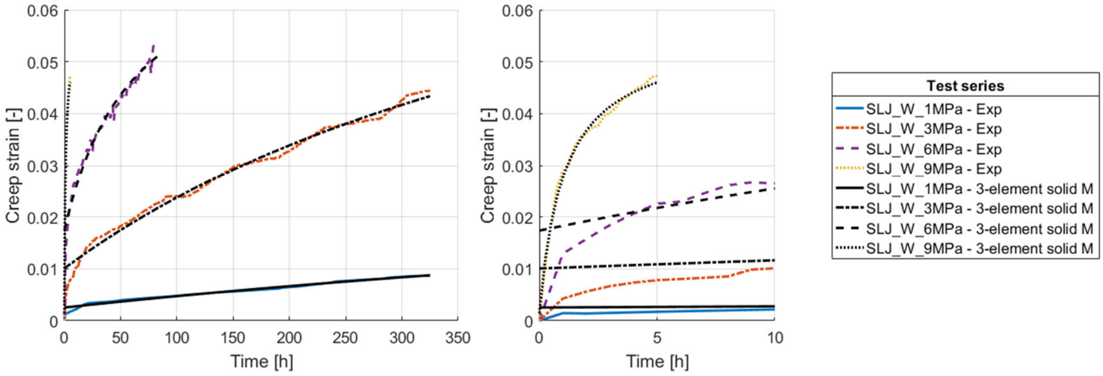

Figure 14: Experimental creep strain and creep strain simulated using Maxwell three element solid models for specimens subjected to loads of 1 MPa, 3 MPa, 6 MPa and 9 MPa in 40°C distilled water. For a colour version of this figure, the reader is referred to the online version

4.2.2 Kelvin-Voigt three-element solid model

The Kelvin-Voigt three-element solid model consists of a spring in series with a Kelvin-Voigt model, as shown in **Figure 15** This model makes the modeling of instantaneous elongation possible. The constitutive equation of the Kelvin-Voigt three-element solid model can be found by using the constitutive equations of the spring and the Kelvin-Voigt model ($\dot{\varepsilon} + E\varepsilon/\eta = \sigma/\eta$ [1]) and is as follows [1]:

$$\sigma + \frac{\eta_2}{E_1 + E_2}\dot{\sigma} = \frac{E_1 E_2}{E_1 + E_2}\varepsilon + \frac{E_1 \eta_2}{E_1 + E_2}\dot{\varepsilon} \tag{3}$$

This constitutive equation can be rewritten to get the response of the model to a constant stress $\sigma = \sigma_0$, applied at t = 0:

$$\varepsilon = \frac{\sigma(t(E_1 + E_2) + \eta_2)}{E_1 E_2 t + E_1 \eta_2} \tag{4}$$

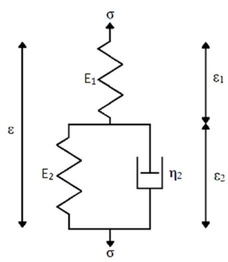

Figure 15: Kelvin-Voigt three-element solid model.

The Kelvin-Voigt three-element solid model (**Figure 15**) has been used to simulate the creep behaviour of the single lap joints. The parameters E_1, E_2 and η_2 of the three-element solid model were estimated using non-linear regression and based on the experimental data. Time was assumed as an independent variable and the creep strain ε_c was assumed as a dependent variable. **Table 3** presents the results from the non-linear regression for the different load levels and environments. The experimental results and the results obtained using the Kelvin-Voigt three-element solid model are compared in **Figure 16** and **Figure 17**.

Table 3: Parameters of the Kelvin-Voigt three-element solid model.

		η_2 [Pa · s]		E_1 [MPa]		E_2 [MPa]		R^2
		Estimate	Standard Error	Estimate	Standard Error	Estimate	Standard Error	
Air	1 MPa	2.20×10^3	129.71	558.71	21.54	291.60	5.66	0.9771
	3 MPa	4.84×10^3	196.98	237.27	3.53	191.21	2.05	0.9845
	6 MPa	2.73×10^3	145.04	485.72	15.94	222.22	2.86	0.9919
	9 MPa	178.78	2.70	5.00×10^3	265.20	33.30	4.08	0.9998
Water	1 MPa	4.26×10^4	1.23×10^3	393.66	6.33	29.76	3.56	0.9847
	3 MPa	1.87×10^4	472.32	297.94	5.91	32.68	1.30	0.9889
	6 MPa	6.36×10^3	476.93	345.73	12.92	101.32	4.48	0.9819
	9 MPa	176.84	25.41	6.52×10^3	9.45×10^3	166.35	4.40	0.9942

Table 3 shows that the parameters η_2, E_1 and E_2 for the Kelvin-Voigt three-element solid model show similar behaviour when compared to the parameters for the Maxwell three-element solid model. For η_2 the same behaviour can be observed as in **Table 2** the E_1 values in **Table 3** show the same pattern as the E_2 values in **Table 2** and the E_2 values in **Table 3** show the same development as the E_1 values in **Table 2**. **Table 3**, **Figure 16** and **Figure 17** show that the Maxwell three-element solid model was able to give an accurate representation of the creep strain of the single lap joint specimens.

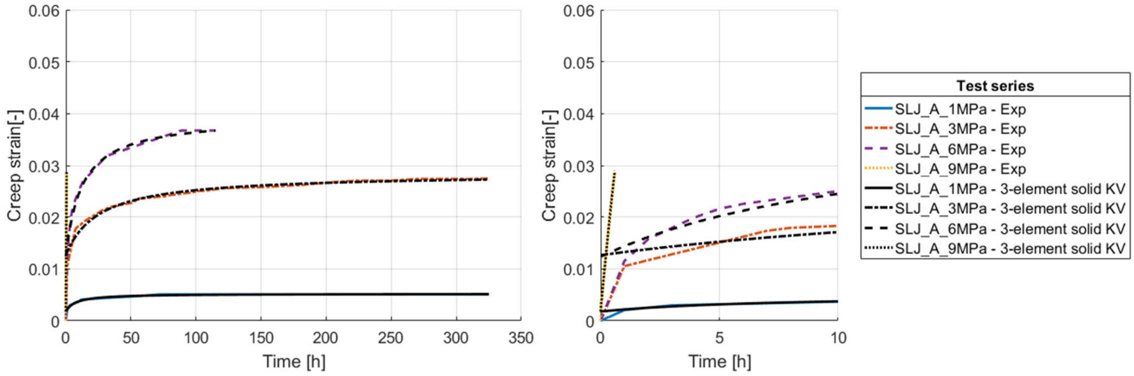

Figure 16: Experimental creep strain and creep strain simulated using Kelvin-Voigt three element solid models for specimens subjected to loads of 1 MPa, 3 MPa, 6 MPa and 9 MPa in 40°C air. For a colour version of this figure, the reader is referred to the online version of this journal.

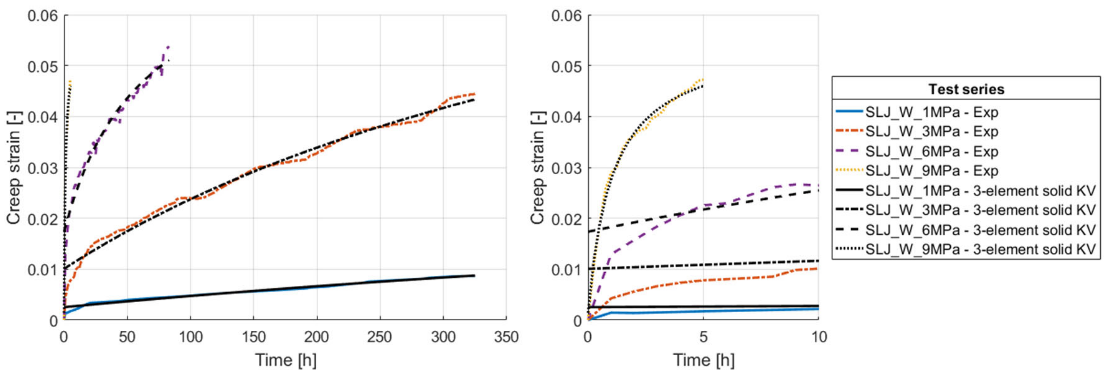

Figure 17: Experimental creep strain and creep strain simulated using Kelvin-Voigt three element solid models for specimens subjected to loads of 1 MPa, 3 MPa, 6 MPa and 9 MPa in 40°C distilled water. For a colour version of this figure, the reader is referred to the online version of this journal.

5 Discussion

5.1 Experimental Results

The experimental results show that an increase in load level resulted in an increase in the instantaneous strain and in the creep strain rate. This is in line with observations from literature, e.g. in Springer & Wang [4], Dean [9] and Zehsaz et al. [17]. Also, the creep strain was found to be larger for specimens loaded in water than for specimens loaded in air, as was found in previous studies, e.g. by Dean [9], Springer et al. [4], Papanicolaou et al. [2] and Farshad & Necola [7]. However, the current study also found that the influence of moisture on the creep strain was dependent on the moisture percentage in the adhesive for load levels of 1 MPa, 3 MPa and 9 MPa. At low moisture concentrations creep is suppressed while at higher moisture concentrations creep is promoted. Heshmati [21] mentions that stable adhesive/steel bonds can benefit from small amounts of moisture through the decrease of peak stresses by the distribution of stresses over a larger area because of the plasticized adhesive. Due to the short time durations of the current study the moisture concentration is however still relatively low at the end of the experiment while the strengthening is only observed at the start. Additionally, no mention of this strengthening phenomenon has been found in literature on creep. This can partly be explained by creep experiments normally being conducted on much larger time scales. In experimental work described in literature the creep deformation might not even have been recorded, especially considering the short time durations regarded in this study. Additionally, the influence of moisture on the creep response is often determined using specimens that have been subjected to moisture for a predefined time or until saturation before testing, e.g. by Papanicolaou et al. [2], Farshad & Necola [7] and Feng et al. [8]. This leads to test conditions that are different than in the current study, in which unaged specimens were subjected to combined moisture and loading.

Literature does however give a possible explanation for the phenomenon described in this study (creep suppression at low moisture concentrations and creep promotion at higher moister concentrations). Colombini et al. [22] mention that the water diffusion and epoxy-water interactions happen mainly under two phenomena. The first phenomenon is the bonding between water molecules and hydrophilic functional groups of macromolecules as the water diffuses through the polymer. This bonding of the water molecules and macromolecules can result in a temporary strengthening of the network. The second phenomenon is the residing of diffused water in the free volume of the material, where it acts as a plasticizer. The contribution of this second phenomenon is considered to be larger than the first phenomenon. The behaviour found in this study suggests that both of these processes occur. Initially, when the water is starting to diffuse into the adhesive the bonding of the water molecules and macromolecules temporarily strengthens the adhesive, resulting in a creep deformation that is initially lower in water conditions than in air conditions. As the water diffuses further into the adhesive, the plasticizing effect of the water residing in the free volume becomes stronger, resulting in a larger strain rate for water conditions than for air conditions.

5.2 Analytical Model

The results showed that both the Maxwell three-element solid model and the Kelvin-Voigt three-element solid model were able to give a good representation of the creep behaviour. Both models gave identical creep representations while having different values for the individual elements. For the single lap joint specimens loaded in water and air, there is no advantage in using one model or the other.

The models are unable to predict the time component of the instantaneous strain, i.e., the short time duration between zero strain and the instantaneous strain value. However, **Figure 13** and **Figure 16** show that for single lap joints loaded in air the models give a good representation of the magnitude of the instantaneous strain. Both the three element Maxwell and the three element Kelvin-Voigt model are unable to predict the magnitude of the instantaneous strain of the single lap joints loaded in water at 1 MPa, 3 MPa and 6 MPa. **Figure 14** and **Figure 17** show that the models give an overestimate of the instantaneous strain, which also results in a misrepresentation of the primary creep phase. This can be explained by two relaxation processes contributing to the creep behaviour of the specimens loaded in water, as described by Dean [9]. Of these two relaxation processes the short-term process is sensitive to the moisture concentration. The models that were used in this study cannot account for these different relaxation processes, resulting in a misrepresentation of the short-term creep behaviour in specimens loaded in water. The three element Maxwell model and the three element Kelvin-Voigt model correctly capture the long-term creep behaviour of single lap joints loaded in both air and water.

6 Conclusions

The present study investigated the influence of combined loading and moisture absorption on the creep strain of a adhesively bonded steel single lap joints. The main conclusions of the study can be summarized as follows:

1. An increase in the load level results in an increase in the instantaneous strain and in the creep strain rate for single lap joints loaded in air and in water.
2. Single lap joints loaded in air generally experience a lower creep strain than single lap joints loaded in water.
3. The creep behaviour of single lap joints loaded at 1 MPa, 3 MPa and 9 MPa (respectively ±5%, 15% and 45% of the lap shear strength) in water is dependent on the moisture concentration in the adhesive layer. At low moisture concentrations creep is suppressed while at higher moisture concentrations creep is promoted. This results in a lower instantaneous strain and a higher strain rate for specimens subjected to combined moisture and loading. The observed behaviour is attributed to different epoxy-water interactions being dominant at different moisture concentrations. At low moisture concentrations the dominant process is related to water molecules bonding to hydrophilic functional groups of the macromolecules, which results in a

temporary strengthening of the epoxy. As the water diffuses further in the epoxy the plasticizing effect of the water residing in the free volume of the material is dominant, thereby decreasing the creep resistance.

4. The three-element solid models were able to give a general correct representation of the creep behaviour of single lap joint specimens loaded in water and air at all tested load levels.
5. The three-element solid models are unable to predict the time component of the instantaneous strain. For single lap joints loaded in air both the three element Maxwell model and the three element Kelvin-Voigt model gives a good representation of the magnitude of the instantaneous strain. However, for single lap joints loaded in water the models give an overestimate of the magnitude of instantaneous strain, which also results in a misrepresentation of the primary creep phase. The models could not account for the short-term relaxation process that is dependent on the moisture concentration. The long-term creep behaviour of both the single lap joints loaded in air and water is however correctly captured by the models.

References

[1] G.C. Papanicolaou and S.P. Zaoutsos. Viscoelastic constitutive modeling of creep and stress relaxation in polymers and polymer matrix composites. In Rui Mirand Guedes, editor, *Creep and Fatigue in Polymer Matrix Composites*, pages 3–47. Woodhead Publishing Limited, Cambridge, 2011.

[2] G. C. Papanicolaou, A. G. Xepapadaki, and D. S. Zarouchas. Effect of water uptake on creep behaviour of glass-epoxy composites. *Plastics, Rubber and Composites*, 38(2):72–79, 2009.

[3] I. Ashcroft and P. Briskham. Designing adhesive joints for fatigue and creep load conditions. In David A. Dillard, editor, *Advances in Structural Adhesive Bonding*, pages 469–515. Woodhead Publishing Limited, Cambridge, 2010.

[4] George S Springer and Tony K Wang. Creep, Strength and Moisture Absorption of Adhesive Bonded FRP Joints. *Journal of Reinforced Plastics and Composites*, 4(2):212–225, 1985.

[5] E.P. Gellert and D.M. Turley. Seawater immersion ageing of glass-fibre reinforced polymer laminates for marine applications. *Composites Part A: Applied Science and Manufacturing*, 30(11):1259–1265, nov 1999.

[6] R.M. Guedes, Alcides Sá, and Hugo Faria. Influence of moisture absorption on creep of GRP composite pipes. *Polymer Testing*, 26(5):595–605, aug 2007.

[7] M. Farshad and A. Necola. Effect of aqueous environment on the long-term behavior of glass fiber-reinforced plastic pipes. *Polymer Testing*, 23(2):163–167, 2004.

[8] C.-W. Feng, C.-W. Keong, Y.-P. Hsueh, Y.-Y. Wang, and H.-J. Sue. Modeling of long-term creep behavior of structural epoxy adhesives. *International Journal of Adhesion and Adhesives*, 25(5):427–436, 2005.

[9] G. Dean. Modelling non-linear creep behaviour of an epoxy adhesive. *International Journal of Adhesion and Adhesives*, 27(8):636–646, 2007.

[10] Huntsman. Araldite ® 2015 - Technical Data Sheet, 2015.

[11] Momentive. Silquest A-187 - Technical Data Sheet, 2018.

[12] M. L. Abel, R. D. Allington, R. P. Digby, N. Porritt, S. J. Shaw, and J. F. Watts. Understanding the relationship between silane application conditions, bond durability and locus of failure. *International Journal of Adhesion and Adhesives*, 26(1-2):2–15, 2006.

[13] A. Zafar, F. Bertocco, J. Schjødt-Thomsen, and J. C. Rauhe. Investigation of the long term effects of moisture on carbon fibre and epoxy matrix composites. *Composites Science and Technology*, 72(6):656–666, 2012.

[14] C.M. de Zeeuw. The behaviour of steel bonded joints under hygrothermal and creep loadings. Master's thesis, Delft University of Technology, jan 2018.

[15] Nihat Özkaya Margareta Nordin, David Goldsheyder, and Dawn Leger. *Fundamentals of biomechanics: equilibrium, motion, and deformation*. Springer Science & Business Media, 2012.

[16] E. Ferrier, L. Michel, B. Jurkiewiez, and P. Hamelin. Creep behavior of adhesives used for external FRP strengthening of RC structures. *Construction and Building Materials*, 25(2):461–467, 2011.

[17] Mohammad Zehsaz, Farid Vakili-Tahami, and Mohammad- Ali Saeimi-Sadigh. Modified creep constitutive equation for an epoxy-based adhesive with nonlinear viscoelastic behavior. *The Journal of Strain Analysis for Engineering Design*, 50(1):4–14, 2015.

[18] H.L. Groth. Viscoelastic and viscoplastic stress analysis of adhesive joints. *International Journal of Adhesion and Adhesives*, 10(3):207–213, 1990.

[19] Mohammad Shishesaz and Arash Reza. The Effect of Viscoelasticity of Polymeric Adhesives on Shear Stress Distribution in a Single-Lap Joint. *The Journal of Adhesion*, 89(11):859–880, nov 2013.

[20] Alan S. Wineman and K.R. Rajagopal. Constitutive Equations for One-Dimensional Response of Viscoelastic Materials: Mechanical Analogs. In *Mechanical Response of Polymers: An Introduction*, pages 28–53. Cambridge University Press, Cambridge, 2000.

[21] Mohsen Heshmati. Hygrothermal durability of adhesively bonded frp/steel joints. 2015.

[22] Didier Colombini, J J Martinez-Vega, and Gérard Merle. Influence of hydrothermal ageing and thermal treatments on the viscoelastic behavior of DGEBA-MCDEA epoxy resin. *Polymer Bulletin*, 48:75–82, 2002.

A Data

Table 4: Mean instantaneous strain and strain rate for specimens loaded at 1 MPa, 3 MPa, 6 MPa and 9 MPa in air and distilled water.

Test series	ε_0 [-]	$\dot{\varepsilon}$ [h^{-1}]
SLJ_A_1MPa - Exp	2.060×10^{-3}	3.175×10^{-8}
SLJ_A_3MPa - Exp	1.053×10^{-2}	1.452×10^{-5}
SLJ_A_6MPa - Exp	1.150×10^{-2}	5.821×10^{-5}
SLJ_A_9MPa - Exp	-	-
SLJ_W_1MPa - Exp	1.461×10^{-3}	1.802×10^{-5}
SLJ_W_3MPa - Exp	4.272×10^{-3}	9.726×10^{-5}
SLJ_W_6MPa - Exp	1.291×10^{-2}	3.394×10^{-4}
SLJ_W_9MPa - Exp	-	4.370×10^{-3}

B Complete creep strain graphs

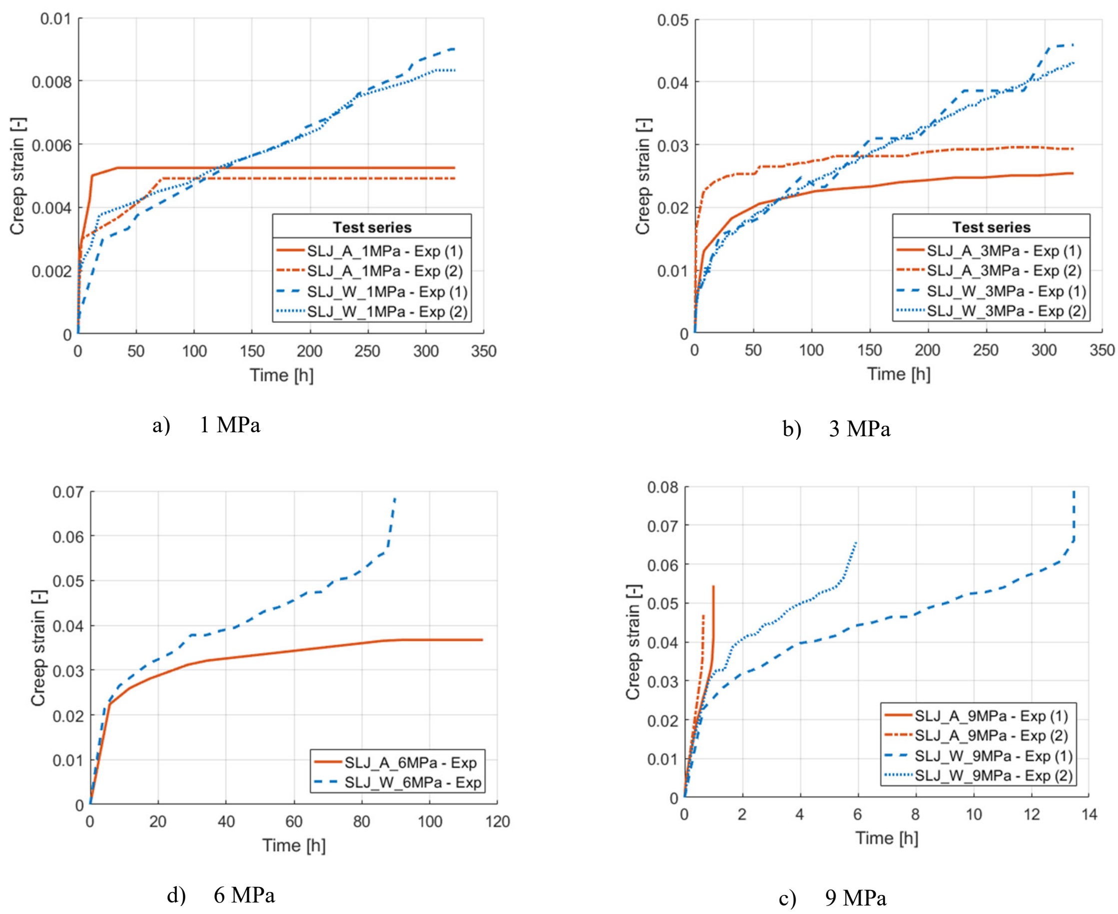

Figure 18: Complete creep strain graphs for specimens loaded at 1 MPa, 3 MPa, 6 MPa and 9 MPa. For a colour version of this figure, the reader is referred to the online version of this journal